Planta (2014) 240:77–89
DOI 10.1007/s00425-014-2065-7

ORIGINAL ARTICLE

# *Arabidopsis* Bax inhibitor-1 promotes sphingolipid synthesis during cold stress by interacting with ceramide-modifying enzymes

**Minoru Nagano · Toshiki Ishikawa · Yoshie Ogawa · Mitsuru Iwabuchi · Akari Nakasone · Ko Shimamoto · Hirofumi Uchimiya · Maki Kawai-Yamada**

Received: 24 December 2013 / Accepted: 13 March 2014 / Published online: 1 April 2014


**Abstract** Bax inhibitor-1 (BI-1) is a widely conserved cell death suppressor localized in the endoplasmic reticulum membrane. Our previous results revealed that *Arabidopsis* BI-1 (AtBI-1) interacts with not only *Arabidopsis* cytochrome $b_5$ (Cb5), an electron transfer protein, but also a Cb5-like domain (Cb5LD)-containing protein, *Saccharomyces cerevisiae* fatty acid 2-hydroxylase 1, which 2-hydroxylates sphingolipid fatty acids. We have now found that AtBI-1 binds *Arabidopsis* sphingolipid Δ8 long-chain base (LCB) desaturases AtSLD1 and AtSLD2, which are Cb5LD-containing proteins. The expression of both *AtBI-1* and *AtSLD1* was increased by cold exposure. However, different phenotypes were observed in response to cold treatment between an *atbi-1* mutant and a *sld1sld2* double mutant. To elucidate the reasons behind the difference, we analyzed sphingolipids and found that unsaturated LCBs in *atbi-1* were not altered compared to wild type, whereas almost all LCBs in *sld1sld2* were saturated, suggesting that AtBI-1 may not be necessary for the desaturation of LCBs. On the other hand, the sphingolipid content in wild type increased in response to low temperature, whereas total sphingolipid levels in *atbi-1* were unaltered. In addition, the ceramide-modifying enzymes *AtFAH1, sphingolipid base hydroxylase 2* (*AtSBH2*)*, acyl lipid desaturase 2* (*AtADS2*) and *AtSLD1* were highly expressed under cold stress, and all are likely to be related to AtBI-1 function. These findings suggest that AtBI-1 contributes to synthesis of sphingolipids during cold stress by interacting with AtSLD1, AtFAH1, AtSBH2 and AtADS2.

**Keywords** *Arabidopsis* · BI-1 · Cold stress · Cytochrome $b_5$ · SLD · Sphingolipid

**Abbreviations**

| | |
|---|---|
| ADS | Acyl lipid desaturase |
| BI-1 | Bax inhibitor-1 |
| BiFC | Bimolecular fluorescence complementation |
| BLAST | Basic local alignment search tool |
| CaMV | Cauliflower mosaic virus |
| Cb5 | Cytochrome $b_5$ |
| Cb5LD | Cytochrome $b_5$-like domain |
| Cer | Ceramide containing non-hydroxy fatty acid |
| COR | Cold-responsive |
| CYP83A1 | Cytochrome P450 83A1 |
| ER | Endoplasmic reticulum |
| FAD | Flavin adenine dinucleotide |
| FAH | Fatty acid 2-hydroxylase |

Dedicated to K. Shimamoto who passed away on September 28, 2013.

M. Nagano and T. Ishikawa contributed equally to this work.

**Electronic supplementary material** The online version of this article (doi:10.1007/s00425-014-2065-7) contains supplementary material, which is available to authorized users.

M. Nagano · K. Shimamoto
Graduate School of Biological Science, Nara Institute of Science and Technology, 8916-5, Takayama, Ikoma 630-0192, Japan

T. Ishikawa · M. Iwabuchi · A. Nakasone · M. Kawai-Yamada (✉)
Graduate School of Science and Engineering, Saitama University, 255 Shimo-Okubo, Sakura-ku, Saitama 338-8570, Japan
e-mail: mkawai@mail.saitama-u.ac.jp

Y. Ogawa
Institute of Molecular and Cellular Biosciences, University of Tokyo, 1-1-1 Yayoi, Bunkyo-ku, Tokyo 113-0032, Japan

H. Uchimiya · M. Kawai-Yamada
Institute for Environmental Science and Technology, Saitama University, 255 Shimo-Okubo, Sakura-ku, Saitama 338-8570, Japan

| | |
|---|---|
| FOA | Fluoroorotic acid |
| GCS | Glucosylceramide synthase |
| GIPC | Glycosylinositolphosphoceramide |
| GlcCer | Glucosylceramide |
| hCer | Ceramide containing 2-hydroxy fatty acid |
| LC–MS/MS | Liquid chromatography–tandem mass spectrometry |
| Moco | Molybdenum-pterin cofactor |
| MRM | Multiple-reaction monitoring |
| MS | Murashige and Skoog |
| NIA | Nitrate reductase |
| PCD | Programmed cell death |
| RLF | Reduced lateral root formation |
| RT-PCR | Reverse transcription polymerase chain reaction |
| SBH | Sphingolipid base hydroxylase |
| SLD | Sphingolipid Δ8 desaturase |
| suY2H | Split-ubiquitin yeast two-hybrid |
| VLCFA | Very long chain fatty acid |
| WT | Wild type |

## Introduction

Bax inhibitor-1 (BI-1) was first identified as a suppressor of cell death induced by Bax, a proapoptotic member of the Bcl-2 family in mammals, by screening a human cDNA library in yeast cells (Xu and Reed 1998). Although no orthologs of Bax have been found in plants, BI-1 is widely conserved in plants such as *Arabidopsis*, rice, tobacco and barely (Ishikawa et al. 2011). Plant BI-1 is an endoplasmic reticulum (ER) protein with approximately seven transmembrane domains; the coiled-coil domain at its C-terminus is essential for its function (Kawai et al. 1999; Kawai-Yamada et al. 2001, 2004). Overexpression of *Arabidopsis* BI-1 (AtBI-1) in tobacco BY-2 cells or rice confers resistance to oxidative stresses such as hydrogen peroxide ($H_2O_2$) or menadione (Kawai-Yamada et al. 2004; Ishikawa et al. 2010, 2013). In addition, expression of *AtBI-1* is increased by pathogen infection, and AtBI-1 participates in decreased susceptibility to *Magnaporthe grisea* elicitor, the fungal toxin fumonisin B1 and infection by *Pseudomonas syringae* possessing *Avr*Rpt2 (Sanchez et al. 2000; Matsumura et al. 2003; Watanabe and Lam 2006; Kawai-Yamada et al. 2009). In barley, BI-1 is related to infection by pathogens such as *Blumeria graminis* f. sp. *tritici*, *Botrytis cinerea*, and powdery mildew (Eichmann et al. 2004, 2010 ; Imari et al. 2006). Furthermore, BI-1 controls responses to carbon starvation, freezing stress, heat shock, ER stress and methyl jasmonate-induced senescence (Bolduc and Brisson 2002; Chae et al. 2003, 2004 ; Watanabe and Lam 2006, 2008; Yue et al. 2012). Therefore, BI-1 plays an important role in regulation of various abiotic and biotic responses in plants. However, studies explaining the molecular mechanism of BI-1-mediated resistance are limited in plants.

To understand this machinery, we explored factors interacting with AtBI-1. We first identified calmodulin as an interactor with AtBI-1, and found that AtBI-1 is involved in ion homeostasis (Ihara-Ohori et al. 2007). Moreover, we revealed that AtBI-1 directly interacts with *Arabidopsis* cytochrome $b_5$ (AtCb5) in the ER membrane (Nagano et al. 2009). Cb5 is an electron transfer protein that possesses a heme-binding domain in its N-terminal cytosolic region and a single transmembrane domain at its C-terminus (Zhao et al. 2003). In *Arabidopsis*, there are four Cb5s (AtCb5-B, -C, -D and -E) in the ER membrane and all of them bind to AtBI-1 (Maggio et al. 2007; Nagano et al. 2009). Furthermore, we demonstrated that AtBI-1 interacts with sphingolipid fatty acid 2-hydroxylases AtFAH1 and AtFAH2 via AtCb5 (Nagano et al. 2009, 2012). This ternary complex increases the synthesis of sphingolipids containing 2-hydroxy fatty acids, leading to the suppression of oxidative stress-induced cell death. On the other hand, a yeast counterpart of AtFAHs, *Saccharomyces cerevisiae* FAH1 (ScFAH1), possesses a Cb5-like domain (Cb5LD) at its N-terminus, and direct binding to AtBI-1 has been confirmed using a split-ubiquitin yeast two-hybrid (suY2H) system (Nagano et al. 2009). These results suggest that AtBI-1 regulates the resistance to various stresses by interaction with not only Cb5-interacting proteins but also Cb5LD-containing proteins. In *Arabidopsis*, there are five Cb5LD-containing proteins, and we expect that AtBI-1 also interacts with and regulates these proteins. Here we describe novel interactors, the sphingolipid Δ8 desaturases AtSLD1 and AtSLD2, and provide evidence for their participation in sphingolipid synthesis during cold treatment through regulation of ceramide-modifying enzymes.

## Materials and methods

### Plant materials and cold treatment

The Columbia (Col-0) ecotype of *Arabidopsis thaliana* (L.) Heynh was used in this study. T-DNA insertion mutants were obtained from the Salk Institute (*atsld1*, SALK_010384) and the GABI-Kat collection (*atsld2*, line 080E07; *atbi1-1*, line 117B05). Plants were cultivated in soil at 23 °C under continuous light (60 μmol/$m^2$/s). For cold treatment, 3-week-old plants were transferred to 4 °C under continuous light and no decrease in fresh weight by water loss was detected in any lines 3 days after cold exposure. Rosette leaves were harvested, frozen in liquid nitrogen and stored at −80 °C until use. For measurement of root elongation, plants were cultured on half-strength Murashige and Skoog (MS) medium containing 1 %

sucrose. Plants were placed vertically at 23 °C under continuous light and transferred to 4 °C 7 days after germination. Root length was measured before and 10 days after cold treatment to evaluate relative root elongation.

### suY2H system

Plasmid vectors and yeast cells were kindly provided by Dr. Ralph Panstruga and Dr. I. E. Somssich. The method using a suY2H system in this study was described in Nagano et al. (2009). pMet-AtBI-1, used as bait vector, was constructed previously (Ihara-Ohori et al. 2007). The coding regions of *AtNIA1*, *AtNIA2*, *AtSLD1*, *AtSLD2* and *RLF* were cloned into vector pCup-NuI-myc to construct the prey vectors. Wild-type yeast cells (W303 strain) were transformed with different combinations of bait and prey constructs, and $His^+Trp^+$ transformants were streaked on a minimal medium containing 0.1 % 5-fluoroorotic acid and were incubated at 30 °C for 4 days. The low Cub-affinity NuA prey variant served as a negative control (Kim et al. 2002).

### BiFC analysis

Plasmids for BiFC analysis were kindly provided by Dr. Nakagawa (Shimane University). *AtSLD1* and *AtSLD2* open reading frames without their stop codons were combined with the BiFC destination vector cYFP-pUGW2 (Nakagawa et al. 2007) by the Gateway system to generate the respective cYFP (amino acids 175–239) C-terminal fusion constructs, AtSLD1-cYFP and AtSLD2-cYFP. Similarly, an AtBI-1-nYFP fusion protein with nYFP (amino acids 1–174) at its C-terminus was generated using the destination vector nYFP-pUGW2 (Nakagawa et al. 2007). The plasmid DNA was introduced into onion epidermal cells by particle bombardment with a helium-driven particle accelerator (GIE-3 IDERA; Tanaka). The BiFC signal was analyzed using a confocal laser microscope (TCS-SP5; Leica). In this system, a 514-nm Ar laser was used for the excitation of YFP. A 543-nm He/Ne laser was also used for DsRed. Emission signals were detected using a 515/30-nm filter for YFP, and a 590/70 or 570-nm long-pass filter for DsRed.

### FRET-APB analysis

The coding regions of *AtSLD1* and *AtSLD2* were, respectively, cloned into the pEarleyGate101 vector to construct AtSLD1-YFP and AtSLD2-YFP (Earley et al. 2006). AtBI-1-CFP was constructed previously (Nagano et al. 2009). CFP excitation is at 442 nm. Plasmid DNA was introduced into onion epidermal cells by particle bombardment with a helium-driven particle accelerator (GIE-3 IDERA; Tanaka).

Confocal microscopy was carried out with a Leica TCS-SP5 microscope. FRET acceptor photobleaching was used for FRET measurements according to the instructions provided by the manufacturer. YFP was photobleached in a region 4–8 μm in diameter, by 2–5 scans with a 514 nm laser set at 100 % power. CFP fluorescence intensity was quantified before donor (d1) and after donor (d2) acceptor photobleaching along with the background fluorescence intensity (bk), and FRET efficiency was determined using the equation: $[(d2 - bk) - (d1 - bk)]/(d2 - bk)$.

### RT-PCR analysis

Total RNA was extracted from *Arabidopsis* rosette leaves using an RNeasy Plant Mini Kit (Qiagen) and cDNA was synthesized using a High-Capacity cDNA Reverse Transcription Kit (Applied Biosystems) according to the instructions provided by the manufacturers. Primer sequences used for RT-PCR analyses are listed in Suppl. Table S1.

### Lipid preparation

For LC–MS/MS analysis, sphingolipids were extracted from homogenized rosette leaves (300 mg fresh weight) and treated with methylamine to remove glycerolipids as described by Markham et al. (2006). During extraction, an internal standard mixture consisting of d18:1-c12:0 ceramide (0.1 nmol for Cer), d18:1-h12:0 ceramide (0.1 nmol for hCer), d18:1-c12:0 GlcCer (1 nmol for GlcCer) and d17:1-c12:0 sphingosyl phosphatidylethanolamine (2 nmol for GIPC) was added. All standard lipids were purchased form Avanti Polar Lipids. The dried extract was resuspended in 1 mL THF/methanol/water (2:1:2, by vol.) containing 0.1 % formic acid and 10 μL was analyzed by LC–MS/MS.

### LC–MS/MS analysis of sphingolipids

Sphingolipids were quantified using an LCMS-8030 system (Shimadzu). Analytical conditions described by Markham and Jaworski (2007) were used with several modifications to fit our system. Chromatographic separation was carried out using an XR-ODSII column (Shimadzu, 2.2 μm, 2.0 mm ID, 75 mm) held at 40 °C with binary elution gradients consisting of THF/methanol/10 mM ammonium formate (3:2:5, by vol.) containing 0.1 % (v/v) formic acid as solvent A and THF/methanol/10 mM ammonium formate (7:2:1) containing 0.1 % (v/v) formic acid as solvent B at a flow rate of 200 μL/min. Each sphingolipid class (Cer, hCer, GlcCer and GIPC) was separately analyzed using solvent concentration gradients as follows: 40–100 % B for Cer and hCer; 30–90 % B for GlcCer; 20–65 % B for GIPC. The starting solvents were changed to the final one for 15 min in a linear fashion, which eluted all analytes.

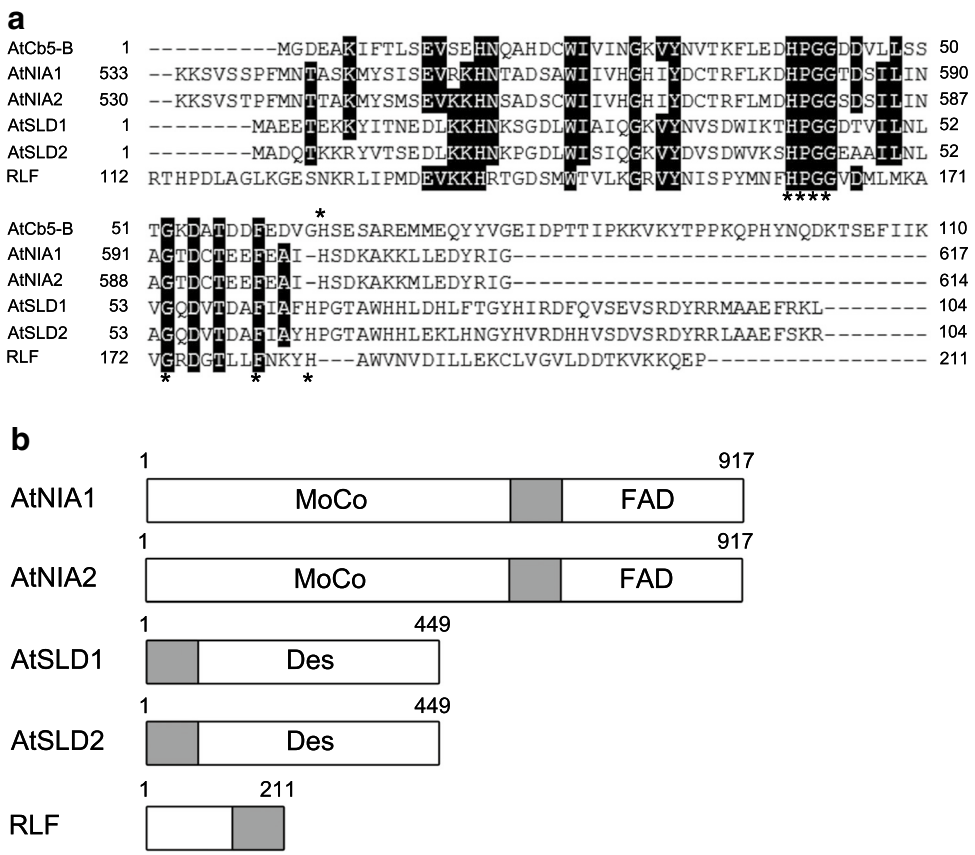


**Fig. 1** The features of Cb5-like domain-containing proteins in *Arabidopsis*. **a** Comparison of amino acid sequences of AtCb5-B and the Cb5-like domain of AtNIA1, AtNIA2, AtSLD1, AtSLD2 and RLF. *Asterisks* indicate conserved amino acids of the Cb5 family. **b** Schematic structures of AtNIA1, AtNIA2, AtSLD1, AtSLD2 and RLF. *Gray boxes* indicate Cb5-like domains. *MoCo* molybdenum pterin cofactor, *FAD* flavin adenine dinucleotide, *Des* desaturase domain

After elution, the column was washed with 100 % B for 1 min and reequilibrated with the appropriate starting solvent for 3 min before the next run.

For quantification of sphingolipid species, transitions of precursor ions $[M + H]^+$ into main product ions were used as precursor/product ion pairs in positive ionization multiple-reaction monitoring mode. For compensation of different MS responses of endogenous sphingolipid species and the internal standards added, sphingolipid classes were fractionated from *Arabidopsis* leaves and MS response factors of each internal standard to endogenous species were determined based on their LCB contents according to Markham and Jaworski (2007). The following conditions were used: capillary voltage, 4.5 kV; desolvation gas flow, 10 L/min; nebulizer gas flow, 0.2 L/min; conversion diode voltage, 6 kV; source temperature, 300 °C; and collision gas flow, 230 kPa. *m*/*z* of precursor/product ions, collision energy and Q1/Q3 pre-bias voltage were optimized for each compound.

### Accession numbers

Sequence data from this article can be found in the *Arabidopsis* Genome Initiative or GeneBank/EMBL databases under Suppl. Table S1 and the following accession numbers: *AtNIA1*, At1g77760; *AtNIA2*, At1g37130; *RLF*, At5g09680; *AtCb5-B*, At2g32720; *AtBI-1*, At5g47120.

## Results

### AtBI-1 interacts with two Δ8-sphingolipid desaturases

BLAST searches based on the amino acid sequence of AtCb5-B revealed that there are five proteins in *Arabidopsis* possessing a heme-binding motif, HPGG, which is broadly conserved in the Cb5 family (Fig. 1a). The two nitrate reductases (AtNIA1 and AtNIA2) are key enzymes in nitrate assimilation, in which they catalyze the reduction of nitrate to nitrite in the cytosol. They contain several prosthetic group binding domains: a molybdenum-pterin cofactor (Moco)-binding domain, a heme-binding Cb5LD domain and a flavin adenine dinucleotide (FAD)-binding domain (Fig. 1b) (Mendel 2011). AtSLD1 and AtSLD2 desaturate the Δ8 position of the long-chain bases (LCBs) of sphingolipids in the ER membrane, and include a Cb5LD at their N-terminus (Fig. 1b) (Sperling et al. 1995; Chen et al. 2012). In addition, one of the proteins, reduced lateral root formation (RLF), is a cytosolic Cb5LD-containing protein that is related to lateral root formation (Fig. 1b)

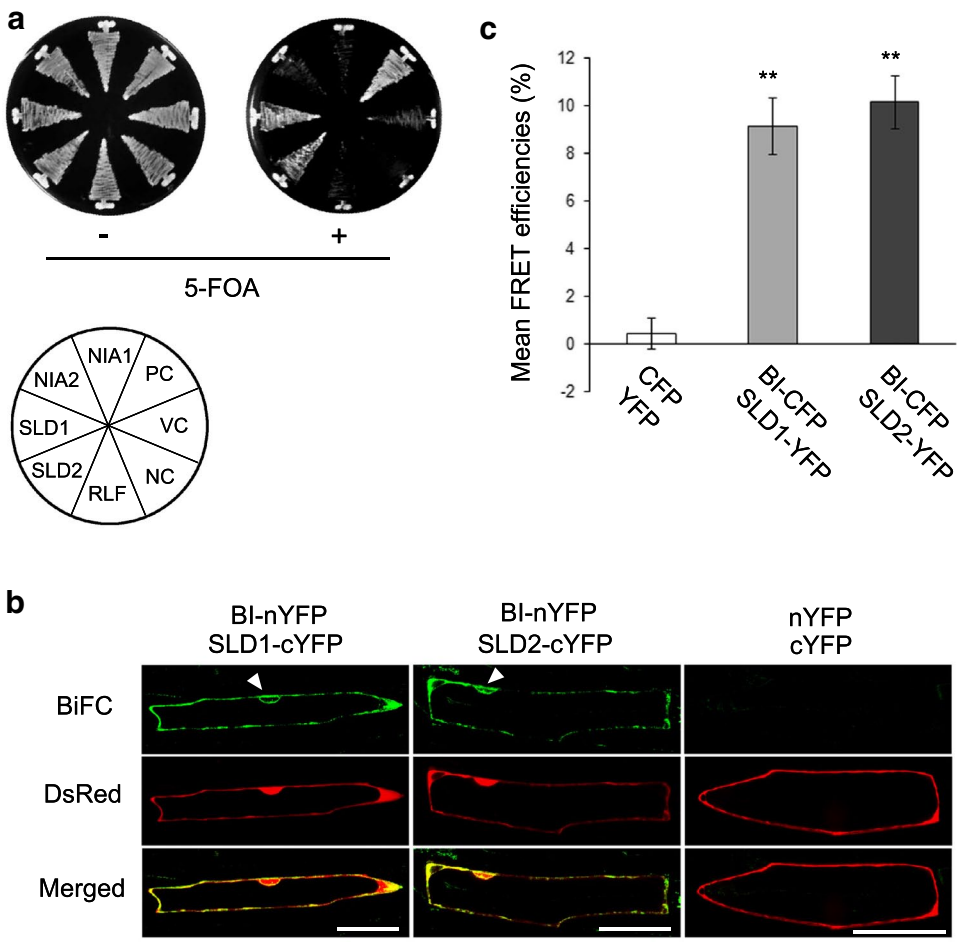


**Fig. 2** Interaction analyses between AtBI-1 and Cb5-like domain-containing proteins. **a** Interactions of AtBI-1 with Cb5-like domain-containing proteins in the suY2H system. Yeast cells containing bait and prey constructs were tested for binding on minimal medium containing 5-fluoroorotic acid (5-FOA). Shown are the growth of each line after 2 days of incubation without 5-FOA and 3 days with 5-FOA at 30 °C. *PC* positive control (pMet-AtBI-1/NuI-AtCb5-B), *VC* vector control (pMet/NuI), *NC* negative control (pMet-AtBI-1/NuI). **b** BiFC visualization in onion epidermal cells with AtBI-1-nYFP/AtSLD1-cYFP, AtBI-1-nYFP/AtSLD2-cYFP and nYFP/cYFP. Images were examined by confocal laser microscopy. *Scale bars* 100 μm. **c** FRET-APB analysis in onion epidermal cells with CFP/YFP, AtBI-1-CFP/AtSLD1-YFP and AtBI-1-CFP/AtSLD2-YFP. Data are mean ± SD FRET efficiency of more than 30 sample sites. *Asterisks* indicate significant differences compared to WT (**$P < 0.01$)

(Ikeyama et al. 2010). Next, we examined whether AtBI-1 interacts with these Cb5LD-containing proteins using a suY2H system (Wittke et al. 1999). When AtBI-1 was used as bait or Cb5LD-containing proteins were used as prey in suY2H system, AtSLD1 and AtSLD2 interacted with AtBI-1 (Fig. 2a). In contrast, no interaction with AtNIA1, AtNIA2 or RLF was detected (Fig. 2a).

To confirm the interaction between AtBI-1 and AtSLDs in plant cells, a bimolecular fluorescence complementation (BiFC) assay was performed. AtBI-1 or AtSLD was fused with the N-terminal region of YFP (nYFP, amino acids 1-174) or with the C-terminal region (cYFP, amino acids 175–239) and driven by cauliflower mosaic virus 35S (CaMV35S) promoter. When AtBI-1-cYFP and AtSLD1-nYFP were co-expressed in onion epidermal cells using particle bombardment, a strong BiFC signal was observed in the cell periphery and perinuclear regions (Fig. 2b, left). The same result was obtained for the combination of AtBI-1-cYFP and AtSLD2-nYFP (Fig. 2b, middle). In contrast, no fluorescent signal was detected for the combination of nYFP and cYFP (Fig. 2b right). In these studies, DsRed driven by the CaMV35S promoter was used as an expression marker of particle bombardment. Taken together with previous studies demonstrating that both AtBI-1 and AtSLDs are localized in the ER membrane (Kawai-Yamada et al. 2004; Chen et al. 2012), these results indicate that AtBI-1 interacts with AtSLD1 and AtSLD2 in the ER.

To further verify these interactions in plant cells, we used a fluorescent resonance energy transfer (FRET)-acceptor photobleaching (APB) analysis. When AtBI-1-CFP was co-expressed with AtSLD1-YFP or AtSLD2-YFP in onion epidermal cells, the respective mean FRET efficiency was 9.15 and 10.2 %, with negative controls (CFP and YFP) showing low FRET efficiency (0.45 %) (Fig. 2c). These data reinforce the results of BiFC assays and suggest that the strength of interaction with AtBI-1 is almost the same for AtSLD1 and AtSLD2.

## *sld1sld2* double mutant is sensitive to cold stress, whereas *atbi-1* exhibits a different phenotype

Sphingolipids are a large family of lipids that are ubiquitous in eukaryotes, and their diversity mainly arises from modifications such as desaturation and hydroxylation of the ceramide moiety, the backbone of sphingolipids containing a LCB and a fatty acid (Markham et al. 2013).

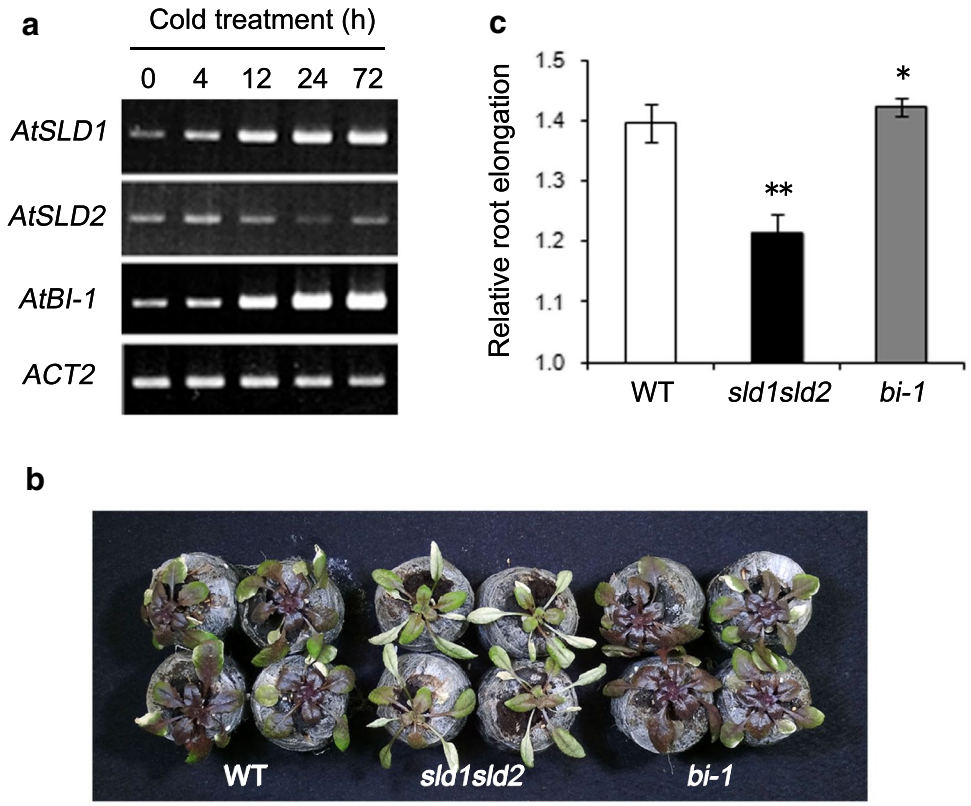


**Fig. 3** Responses to cold treatment in *Arabidopsis sld1sld2* and *atbi-1* mutants. **a** Levels of expression of *AtSLD1*, *AtSLD2* and *AtBI-1* during cold treatment at 4 °C were analyzed by RT-PCR. *Actin2* (*ACT2*) was used as an internal control. **b** Representative phenotype of rosette leaves of WT, *sld1sld2* and *atbi-1* after cold treatment for 4 weeks at 4 °C. **c** Relative root elongation under low temperature. Seven-day-old plants were treated for 10 days at 4 °C and root length was measured before and after treatment. Data are means ± SD ($n = 9$–11). *Asterisks* indicate significant differences between WT and each mutant line (*$P < 0.05$, **$P < 0.01$)

Approximately, 90 % of *Arabidopsis* LCBs contain a *cis* or *trans* double bond at the Δ8 position, and their desaturation is catalyzed by AtSLD1 and AtSLD2 (Chen et al. 2012). Their amino acid sequences are approximately 79 % identical, and both proteins possess Δ8 desaturase activity toward sphingolipid LCBs in yeast cells (Sperling et al. 1998; Chen et al. 2012). In contrast, *AtSLD1* is broadly expressed in all tissues, whereas the expression of *AtSLD2* is limited to flowers and siliques (Chen et al. 2012). In addition, AtSLD1 contributes to Δ8 LCB desaturation in stems, flowers, leaves, siliques and roots, although AtSLD2 has a small effect on desaturation in every tissue, even in flowers and siliques, where *AtSLD2* is highly expressed. Thus, there are functional differences between AtSLD1 and AtSLD2, but they are considered the only enzymes related to Δ8 desaturation of sphingolipid LCBs in *Arabidopsis*.

Moreover, *sld1* mutants and the *sld1sld2* double mutant were hypersensitive to low temperature compared with wild-type (WT) plants (Chen et al. 2012). Thus, we expected a functional relationship between AtSLDs and AtBI-1 in chilling tolerance. When we checked the expression of *AtSLD1* and *AtBI-1* at 4 °C, it was dramatically increased, whereas the expression of *AtSLD2* gradually decreased (Fig. 3a). Next, we compared the effects of cold exposure on AtSLDs and AtBI-1 using knockout mutants. In the experiments described below, we used crosses of the *sld1sld2* double mutants to *sld1* (SALK_010384) and *sld2* (GABI-KAT 080E07), and a lack of expression of both was confirmed (Fig. 5). In addition, an *atbi-1* mutant (GABI-KAT 117B05) was reported in Watanabe and Lam (2006). Neither the *atbi-1* nor the *sld1sld2* mutant exhibited any obvious growth defects under normal conditions (data not shown), but when plants were treated at 4 °C for 4 weeks, *sld1sld2* showed severe chlorosis and low accumulation of anthocyanins, similarly to the result in Chen et al. (2012) (Fig. 3b, middle). However, no such phenotype was observed in the *atbi-1* mutant (Fig. 3b, right). In addition, the growth of *sld1sld2* roots was inhibited at 4 °C, whereas growth of the roots of *atbi-1* was not inhibited or was even slightly stimulated compared with WT (Fig. 3c). These results suggest that although the expression of both *AtSLD1* and *AtBI-1* responds to cold treatment and their effects on cold tolerance differ.

## The amount of sphingolipids increases under low temperature, although the ratio of LCB desaturation is unaltered

To uncover the relationship between AtSLDs and AtBI-1 in sphingolipid synthesis and the difference in cold responses between *sld1sld2* and *atbi-1* mutants, we analyzed the sphingolipid content under low temperature. After WT, *sld1sld2* and *atbi-1* were treated at 4 °C for 0, 24 or 72 h, total sphingolipids were extracted from shoots of each according

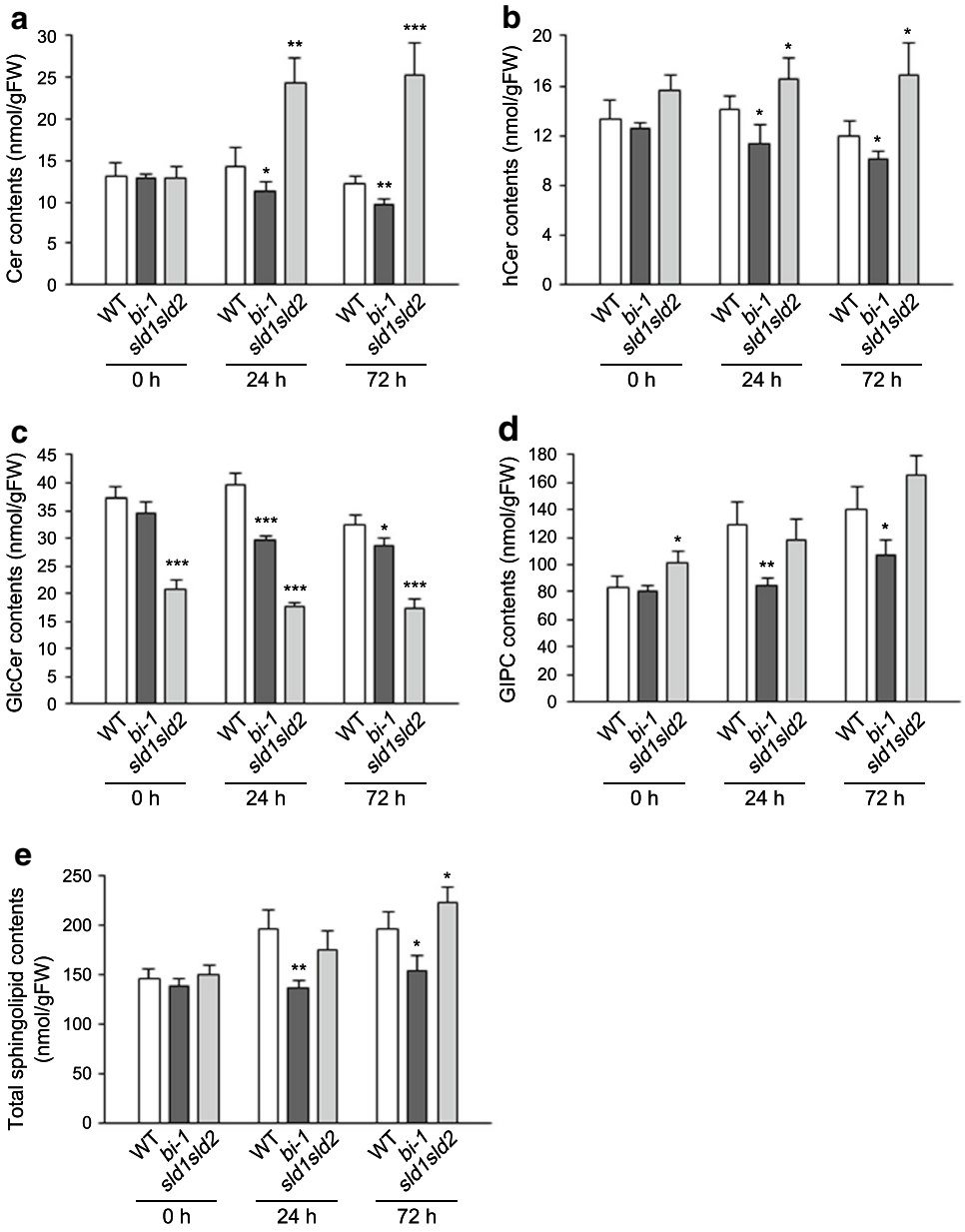


**Fig. 4** Sphingolipid content in *sld1sld2* and *atbi-1* during cold treatment. Sphingolipid content in cold-treated *Arabidopsis* shoots was determined by LC–MS/MS and is shown as total amount of each class (**a** ceramide, **b** hydroxyceramide, **c** GlcCer, **d** GIPC, **e** total sphingolipid). *Asterisks* indicate significant differences compared to WT at each time point (Student's *t* test; $*P < 0.05$, $**P < 0.01$, $***P < 0.001$). See Figure S2 for amounts of individual lipid species

to Markham and Jaworski (2007). We analyzed four major classes of sphingolipids: ceramides containing non-hydroxy fatty acids (Cers), ceramides containing 2-hydroxy fatty acids (hCers), glucosylceramides (GlcCers) and glycosylinositolphosphoceramides (GIPCs) by liquid chromatography–tandem mass spectrometry (LC–MS/MS) (see Suppl. Fig. S1; Summary in Fig. 4). In agreement with the sphingolipidome analysis under normal condition in Chen et al. (2012), a large portion of the LCBs were unsaturated in WT before cold exposure, whereas almost all LCBs were saturated in the *sld1sld2* mutant (Table 1). The small amount of unsaturated LCBs detected in *sld1sld2* was confirmed as d18:1$^{\Delta 4}$ by analysis of liberated LCBs, since LC–MS/MS-based methods cannot distinguish between the double bond positions of d18:1$^{\Delta 8}$ and d18:1$^{\Delta 4}$. Unexpectedly, the ratio of unsaturated LCBs in WT was unchanged by low temperature, although the expression of *AtSLD1* was markedly increased (Table 1; Fig. 3a). Therefore, unsaturated LCBs may be necessary for basic resistance to cold rather than for induced tolerance after cold exposure. In contrast, the LCBs of each sphingolipid species in the *atbi-1* mutant were largely unsaturated at a level similar to that of WT before and after cold treatment (Table 1). This result implies that AtBI-1 is not indispensable for the desaturation of sphingolipid LCBs. In addition, the large difference in extent of LCB desaturation between *sld1sld2* and *atbi-1* is likely responsible for their different phenotypes under cold stress.

**Table 1** Desaturation of LCB moieties of sphingolipid classes during cold treatment

| Class | Plant | Desaturation of LCB moiety (mol %) | | |
|---|---|---|---|---|
| | | 0 h | 24 h | 72 h |
| Ceramide | WT | 71.3 ± 0.6 | 74.0 ± 0.9 | 70.0 ± 4.8 |
| | *sld1sld2* | 1.0 ± 0.3*** | 0.9 ± 0.1*** | 0.9 ± 0.3*** |
| | *bi-1* | 72.4 ± 0.9 | 75.3 ± 1.0 | 75.4 ± 0.9 |
| Hydroxyceramide | Col-0 | 88.6 ± 2.6 | 92.3 ± 1.3 | 92.2 ± 1.6 |
| | *sld1sld2* | 0.6 ± 0.1*** | 1.1 ± 0.2*** | 1.1 ± 0.3*** |
| | *bi-1* | 91.5 ± 0.7 | 94.4 ± 0.6* | 95.1 ± 0.7* |
| GlcCer | Col-0 | 98.1 ± 0.1 | 98.3 ± 0.1 | 98.3 ± 0.1 |
| | *sld1sld2* | 0.6 ± 0.2*** | 0.8 ± 0.1*** | 0.8 ± 0.2*** |
| | *bi-1* | 98.2 ± 0.2 | 98.3 ± 0.1 | 98.4 ± 0.1 |
| GIPC | Col-0 | 85.6 ± 0.2 | 85.1 ± 0.2 | 85.2 ± 0.6 |
| | *sld1sld2* | 0.3 ± 0.1*** | 0.5 ± 0.3*** | 0.5 ± 0.3*** |
| | *bi-1* | 86.1 ± 0.2* | 84.3 ± 0.4* | 85.3 ± 0.4 |
| Total | Col-0 | 89.0 ± 0.2 | 88.2 ± 0.2 | 87.6 ± 0.8 |
| | *sld1sld2* | 0.4 ± 0.1*** | 0.6 ± 0.2*** | 0.6 ± 0.3*** |
| | *bi-1* | 89.3 ± 0.2 | 88.0 ± 0.4 | 88.2 ± 0.4 |

Values are mean ± SD ($n = 4$). Asterisks indicate significant differences (Student's $t$ test; * $P < 0.05$, *** $P < 0.001$). See Suppl. Fig. S2 for whole dataset of sphingolipid measurement

On the other hand, the total amount of sphingolipids increased in WT with increasing GIPC level 24 h after cold treatment and the amount was maintained until 72 h, whereas GlcCer decreased at 72 h after a slight increase at 24 h (Fig. 4). In *sld1sld2*, the GIPC level increased similarly to WT at low temperature, although GlcCer remained at approximately one-third of the amount of WT (Fig. 4). This lower GlcCer level in *sld1sld2* shows the importance of the desaturation of LCBs in the synthesis of GlcCers, as described in Chen et al. (2012). Interestingly, the amount of Cer with C16:0 fatty acid and saturated LCBs was dramatically elevated in response to cold treatment in *sld1sld2*, although hCer also increased to some extent (Suppl. Fig. S1a; Fig. 4a, b). Cer induces programmed cell death (PCD) in plants as well as animals (Berkey et al. 2012), suggesting that abnormal accumulation of Cer by cold treatment in *sld1sld2* results in related phenotypes such as chlorosis (Fig. 3b). By contrast, the level of Cer, hCer and GlcCer in *atbi-1* gradually decreased with cold treatment, and the increase in GIPC level was remarkably slow compared to WT (Fig. 4a–d). Therefore, the amount of each sphingolipid species in *atbi-1* was significantly lower than that in WT after cold exposure (Fig. 4e), suggesting that AtBI-1 contributes to the increase in total content of sphingolipids during cold stress.

### *AtFAH1*, *AtSBH2* and, *AtADS2* as well as *AtSLD1* were markedly expressed in response to cold treatment

To ascertain whether the changes in sphingolipid content in each line during cold treatment are caused by different expression patterns of sphingolipid-related genes, we examined their levels of transcription at 4 °C. When we first checked the AtBI-1 interactors, *AtSLD*s and *AtFAH*s, by semi-quantitative RT-PCR, we observed that expression of *AtSLD1* and *AtFAH1* increased in response to cold treatment in WT, whereas *AtSLD2* and *AtFAH2* decreased (Fig. 5). In *atbi-1* and *sld1sld2*, *AtFAH1* was similarly expressed under low temperature, and *AtSLD1* transcripts also increased in *atbi-1* (Fig. 5). Because AtSLD1 and AtFAH1 are enzymes modifying a ceramide moiety, we also investigated the expression of the *sphingolipid base hydroxylase* (*SBH*) and *acyl lipid desaturase* (*ADS*) genes (Chen et al. 2008; Smith et al. 2013). As shown in Fig. 5, transcript levels of *AtSBH2* and *AtADS2* increased following cold treatment in WT, *sld1sld2* and *atbi-1*, whereas *AtSBH1* and *AtADS1* decreased. In contrast, almost no other genes encoding sphingolipid-related enzymes were upregulated in response to cold treatment in any of the lines (Suppl. Fig. S2). These results suggest that some ceramide-modifying enzymes respond to low temperature and that neither AtSLDs nor AtBI-1 affects their levels of transcription under cold treatment.

Our previous studies revealed that AtBI-1 interacts with AtFAH1 through its interaction with AtCb5 (Nagano et al. 2009, 2012). In addition, AtBI-1 interacts with AtSLD1, which possesses a Cb5LD as shown in Fig. 2. Generally, Cb5 supplies electrons to hydroxylases and desaturases (Schenkman and Jansson 2003), so we hypothesized that AtBI-1 also interacts with AtSBH2 and AtADS2 through AtCb5. When we tested whether AtSBH2 and AtADS2 interact with AtCb5 using our suY2H system, their interaction was confirmed (Fig. 6), leading to the possibility that AtBI-1 interacts with them through an interaction with

AtCb5 like AtFAH1. Taken together with the observed sphingolipids of *atbi-1*, it seems that AtBI-1 may contribute to the increase in sphingolipid content under cold stress by interacting with AtSLD1, AtFAH1, AtSBH2 and AtADS2.

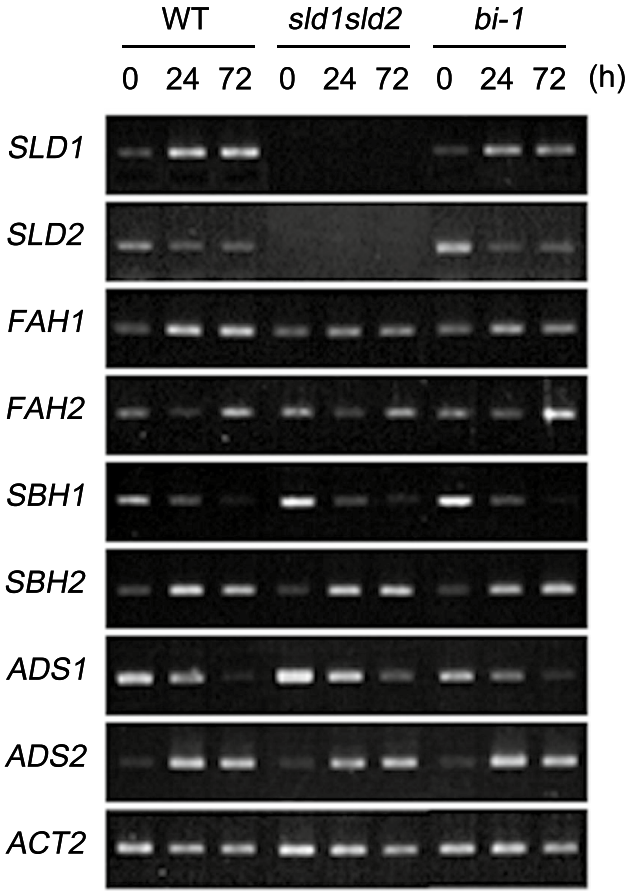


**Fig. 5** Transcription of genes encoding sphingolipid LCB- or fatty acid-modifying enzymes during cold treatment. Levels of expression of *AtSLD1*, *AtSLD2*, *AtSBH1*, *AtSBH2*, *AtFAH1*, *AtFAH2*, *AtADS1* and *AtADS2* in WT, *sld1sld2* and *atbi-1* at 4 °C were analyzed. *ACT2* was used as an internal control

## Discussion

We previously demonstrated that AtBI-1 interacts with not only AtCb5s, but also a yeast Cb5LD-containing protein, ScFAH1 (Nagano et al. 2009). We have now identified AtSLD1 and AtSLD2, which also possess Cb5LDs, as novel interactors with AtBI-1. Interestingly, *Arabidopsis* has three other Cb5LD-containing proteins, AtNIA1, AtNIA2 and RLF. These Cb5LDs of these proteins, which are cytosolic, had comparable sequence identity with AtCb5-B, almost the same as that of the AtSLDs, suggesting that they also interact with AtBI-1. However, none of them interacted with AtBI-1 in the suY2H system. This may be due to their distinct functions. As described above, AtSLD1 and AtSLD2 are sphingolipid Δ8 LCB desaturases. In addition, ScFAH1 is a fatty acid hydroxylase of sphingolipids, and its *Arabidopsis* counterparts lacking a Cb5-like domain, the AtFAHs, interact with AtBI-1 through AtCb5s (Nagano et al. 2009, 2012). In contrast, AtNIA1 and AtNIA2 are nitrate reductases, and RLF is a protein related to lateral root formation, not sphingolipid metabolism. Therefore, AtBI-1 may predominantly interact with sphingolipid-modifying proteins that need to accept electrons from a Cb5 or Cb5-like domain. On the other hand, a recent study has demonstrated from co-immunoprecipitation-based mass spectrometry and FRET analyses that AtBI-1 interacts with cytochrome P450 83A1 (CYP83A1) in the ER membrane (Weis et al. 2013). The CYP family is made up of a wide variety of monooxygenases containing a prosthetic heme group, and CYP83A1 is required for aliphatic glucosinolate biosynthesis (Bak and Feyereisen 2001; Mizutani 2012). Therefore, AtBI-1 could be related to the synthesis of not only sphingolipids but also various metabolites. It will be interesting to determine in which metabolic pathways AtBI-1 is involved.

Chen et al. (2012) reported that the *sld1sld2* mutant exhibits leaf chlorosis, and we have now found that *AtSLD1* is highly expressed in response to low temperature and that root elongation of *sld1sld2* is also affected by cold

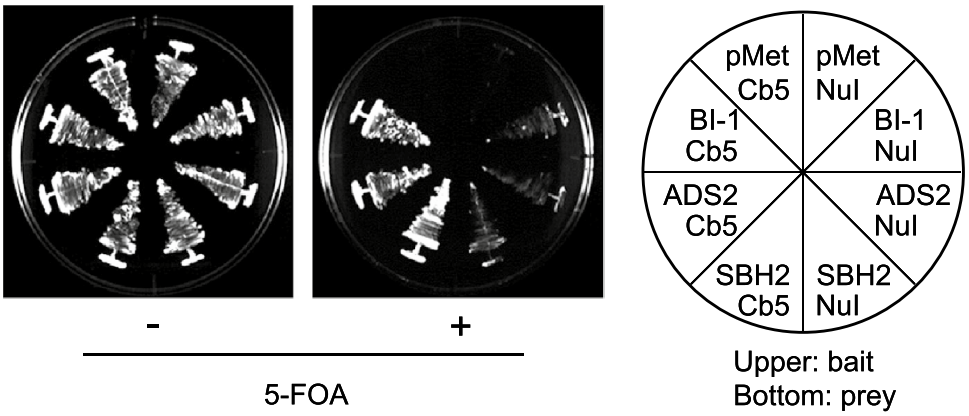


**Fig. 6** Interaction analysis of AtSBH2 and AtADS2 with AtCb5. Interactions of AtSBH2 and AtADS2 with AtCb5 in the suY2H system. Yeast cells containing bait and prey constructs were tested for binding on the minimal medium containing 5-fluoroorotic acid (5-FOA). Shown are the growth of each line after 2 days of incubation without 5-FOA and 3 days with 5-FOA at 30 °C

exposure. This phenotype suggests that desaturation of sphingolipid LCBs is crucial to the plant cold response. However, our sphingolipidome analyses demonstrated that the ratio of unsaturated LCBs is not increased by low temperature in WT plants at all, whereas total sphingolipid content is elevated. These results suggest that sphingolipids with unsaturated LCBs, which reach >90 % of total sphingolipids during normal growth, are essential for natural tolerance to low temperature rather than for induced resistance after cold acclimation.

Fatty acid desaturation plays an essential role in cold resistance (Nishida and Murata 1996; Upchurch 2008). Low temperature decreases the entropy of membranes, resulting in their hardening. Although this membrane rigidification is important for the induction of expression of *cold-responsive* (*COR*) genes, it can also cause collapse of cells and organelles in the subsequent freezing season (Miura and Furumoto 2013). To prevent this, plant cells increase the proportion of polyunsaturated fatty acids such as C18:2 or C18:3 in membrane glycerolipids to recover membrane fluidity. Since sphingolipids are also membrane lipids including unsaturated double bonds in their acyl moieties, their desaturation might participate in cold tolerance determined by membrane properties. In fact, both *sld1sld2* and *ads2* mutants exhibited hypersensitivity to cold stress, as observed in this study and previous reports (Fig. 3; Chen et al. 2012; Chen and Thelen 2013). It is possible that membrane fluidity is decreased by the depletion of sphingolipids with unsaturated LCBs, leading to decreased cold tolerance in *sld1sld2*. In addition, sphingolipidome analysis showed that the amount of C16-Cer was dramatically increased by low temperature in *sld1sld2* mutant. Chen et al. (2008) reported that in the *sbh1sbh2* mutant, which accumulates a large amount of C16-Cer even under normal growth conditions, a severe dwarf phenotype was observed and the expression of PCD-associated genes was greatly enhanced. Furthermore, there are a number of reports that the accumulation of Cers induces cell death in plants (Spassieva et al. 2002; Liang et al. 2003; Townley et al. 2005). Thus, high accumulation of C16-Cer under cold stress in the *sld1sld2* mutant may cause serious damage. In contrast, the accumulation of GlcCers in the *sld1sld2* mutant was very low even in the absence of cold stress. This is, however, unlikely to be related to a cold response, because a decrease in GlcCer due to a reduction in expression of *GlcCer synthase* (*GCS*) reportedly does not affect the cold response in *Arabidopsis*, as described in Chen et al. (2012).

By contrast, the chilling tolerance phenotype of *atbi-1* was different from that of *sld1sld2*, although AtBI-1 interacted with AtSLDs, and both *AtBI-1* and *AtSLD1* were highly expressed during cold exposure. This discrepancy can be explained by their sphingolipid composition. In *atbi-1*, the ratio of unsaturated LCBs was similar to WT regardless of temperature, in contrast to drastic changes in *sld1sld2* (Table 1). This result suggests that AtBI-1 does not affect the ratio of unsaturated LCBs. However, whereas the amounts of sphingolipid species in WT were increased 24 h after cold treatment, the total amount of sphingolipid did not increase in *atbi-1*, suggesting that AtBI-1 contributes to the increase in the amounts of sphingolipids under low temperature. Transcriptional analyses of sphingolipid-related genes showed that their expression was almost unaffected by the deletion of *AtBI-1*. Therefore, under cold stress, AtBI-1 may regulate the activity of sphingolipid-related enzymes, rather than the level of transcription of the corresponding genes. We also found that four genes encoding ceramide-modifying enzymes, *AtFAH1*, *AtSBH2*, *AtADS2* and *AtSLD1*, were highly upregulated in response to low temperature (Figs. 3, 5). AtFAH1 2-hydroxylates sphingolipid fatty acids, especially very long chain fatty acids (VLCFAs), and is related to resistance to oxidative stress by its interaction with AtBI-1 via AtCb5. (Nagano et al. 2009, 2012). AtSBH2 is one of the enzymes that catalyze the C4 hydroxylation of sphingolipid LCBs to synthesize trihydroxy LCBs such as t18:0 and t18:1 (Chen et al. 2008). Although the level of expression of *AtSBH2* is lower than *AtSBH1*, and the contribution of AtSBH2 to hydroxylation is lower than that of AtSBH1, AtSBH2 also plays important roles in C4 hydroxylation and physiological functions because the *sbh1sbh2* double mutant shows more a severe phenotype than the *sbh1* single mutant (Chen et al. 2008). AtADS2 is reported to function not only as a predominant desaturase of sphingolipid VLCFAs, especially for C24 and C26, but also as a palmitic acid desaturase of monogalactosyl diacylglycerol and phosphatidylglycerol (Smith et al. 2013; Chen and Thelen 2013). The elevation of *AtADS2* expression during cold treatment was already described by Fukuchi-Mizutani et al. (1998), and Chen and Thelen (2013) recently demonstrated that an *atads2* mutant showed growth defects under low temperature. Now, we have found that both AtSBH2 and AtADS2 interact with AtCb5-B similarly to AtFAH1. Taken together with earlier reports that both AtSBH2 and AtADS2 are localized in the ER membrane (Chen et al. 2008; Smith et al. 2013; Chen and Thelen 2013), it is possible that both proteins also interact with AtBI-1 through AtCb5, like AtFAH1. The major sphingolipid species in *Arabidopsis* are composed of Δ8-unsaturated trihydroxy LCBs (t18:1) and 2-hydroxylated VLCFAs that are often Δ9 unsaturated: these structures of the ceramide moiety are generated by collaboration of AtSLD, AtFAH, AtSBH and AtADS. Sphingolipidome analysis demonstrated that the amounts of most sphingolipid species containing this typical ceramide moiety were lower in cold-treated *atbi-1* than WT, resulting in a significant decrease in total sphingolipid content (Fig. 4; Suppl. Fig. S1). These results suggest that AtBI-1 assists

in the synthesis of sphingolipids modified by AtSLD1, AtFAH1, AtSBH2 and AtADS2 under cold stress through the interaction with them.

However, the cold-induced increase of sphingolipids does not seem to directly contribute to cold tolerance, since the sphingolipid level of the *atbi-1* mutant is not increased by low temperature, yet it was slightly more tolerant to cold stress than WT (Fig. 3). One speculation is that an increase in sphingolipid content causes a decrease in membrane fluidity, because sphingolipids form a more rigid membrane than glycerolipids (Pata et al. 2010), which is followed by a slight reduction in chilling tolerance in WT plants. Alternatively, the increase in sphingolipid content may affect the formation of membrane microdomains, so-called membrane rafts, which are formed by sphingolipids and sterols mainly in the plasma membrane (Cacas et al. 2012). Because a lot of membrane and membrane-anchored proteins on rafts are considered important for cellular functions, it is possible that cold-responsive proteins are affected by the increase in sphingolipids. In addition, our sphingolipidome analysis showed that the amount of GIPC increased in WT during low temperature, whereas GlcCer had decreased in an opposite manner at 72 h. Although the decrease in GlcCer during cold treatment is consistent with previous studies (Uemura et al. 1995; Minami et al. 2010; Degenkolbe et al. 2012), we have now found that GIPC synthesis is upregulated at an early stage of cold acclimation in WT *Arabidopsis* plants, leading to an increase in total sphingolipid. This evidence indicates that the metabolic flow of the ceramide modification pathway shifts to generate GIPC rather than GlcCer under cold stress, conditions under which cold-induced upregulation of AtBI-1 and the Cb5-interacting enzymes would be involved. It will be interesting to understand why the predominant sphingolipid synthesized during low temperature is GIPC. Furthermore, AtBI-1 might also participate in regulating the sphingolipid level when plants are exposed to other stresses such as oxidative conditions, because AtBI-1 confers resistance to them (Kawai-Yamada et al. 2004; Ishikawa et al. 2010, 2013). Thus, it will also be interesting to reveal the relationship between the regulation of sphingolipid metabolism by AtBI-1 and resistance to various stresses.

**Acknowledgments** Plasmids and strains used for the suY2H system were generously provided by Dr. Ralph Panstruga (Max-Planck Institute, Saabruecken, Germany) and Dr. Imre E. Somssich (Max-Planck Institute). Plasmids used for the BiFC assay were kindly provided by Dr. Tsuyoshi Nakagawa (Shimane University, Japan). We appreciate Dr. Noriko Inada (Nara Institute of Science and Technology, Japan) for technical advice of confocal laser microscopy and FRET analysis. We are grateful to Dr. Ikuo Nishida (Saitama University, Japan) for cold stress analysis and to Dr. Hiroyuki Imai (Konan University, Japan) for lipid analysis. This work was supported by a Grant from the Japan Society for the Promotion of Science (JSPS) through the "Funding Program for Next Generation World-Leading Researchers (NEXT program, to M.K.-Y.)," initiated by the Council for Science and Technology Policy (CSTP), a Grant-in-Aid for JSPS Fellows (to M.N. and T.I.), and a Grant from the Ministry of Agriculture, Forestry and Fishery, Japan (Genomics for Agricultural Innovation, IPG-0014). Minoru Nagano and Toshiki Ishikawa contributed equally to this work.

## References

Bak S, Feyereisen R (2001) The involvement of two p450 enzymes, CYP83B1 and CYP83A1, in auxin homeostasis and glucosinolate biosynthesis. Plant Physiol 127:108–118

Berkey R, Bendigeri D, Xiao S (2012) Sphingolipids and plant defense/disease: the "death" connection and beyond. Front Plant Sci 3:1–22

Bolduc N, Brisson LF (2002) Antisense down regulation of NtBI-1 in tobacco BY-2 cells induces accelerated cell death upon carbon starvation. FEBS Lett 532:111–114

Cacas JL, Furt F, Le Guedard M, Schmitter JM, Bure C, Gerbeau-issot P, Moreau P, Bessoule JJ, Simon-Plas F, Mongrand S (2012) Lipids of plant membrane rafts. Prog Lipid Res 51:272–299

Chae HJ, Ke N, Kim HR, Chen S, Godzik A, Dickman M, Reed JC (2003) Evolutionarily conserved cytoprotection provided by Bax Inhibitor-1 homologs from animals, plants, and yeast. Gene 323:101–113

Chae HJ, Kim HR, Xu C, Bailly-Maitre B, Krajewska M, Krajewski S, Banares S, Cui J, Digicaylioglu M, Ke N, Kitada S, Monosov E, Thomas M, Kress CL, Babendure JR, Tsien RY, Lipton SA, Reed JC (2004) BI-1 regulates an apoptosis pathway linked to endoplasmic reticulum stress. Mol Cell 15:355–366

Chen M, Thelen JJ (2013) *ACYL-LIPID DESATURASE2* is required for chilling and freezing tolerance in *Arabidopsis*. Plant Cell 25:1430–1444

Chen M, Markham JE, Dietrich JG, Jaworski JG, Cahoon EB (2008) Sphingolipid long-chain base hydroxylation is important for growth and regulation of sphingolipid content and composition in *Arabidopsis*. Plant Cell 20:1862–1878

Chen M, Markham JE, Cahoon EB (2012) Sphingolipid Δ8 unsaturation is important for glucosylceramides biosynthesis and low-temperature performance in *Arabidopsis*. Plant J 69:769–781

Degenkolbe T, Giavalisco P, Zuther E, Seiwert B, Hincha DK, Willmitzer L (2012) Differential remodeling of the lipidome during cold acclimation in natural accessions of *Arabidopsis thaliana*. Plant J 72:972–982

Earley KW, Haag JR, Ontes O, Juehne T, Song K, Pikaard CS (2006) Gateway-compatible vectors for plant functional genomics and proteomics. Plant J 45:616–629

Eichmann R, Schultheiss H, Kogel KH, Hückelhoven R (2004) The barley apoptosis suppressor homologue BAX inhibitor-1compromises nonhost penetration resistance of barley to the inappropriate pathogen *Blumeria graminis* f. sp. *tritici*. Mol Plant Microbe Interact 17:484–490

Eichmann R, Bischof M, Weis C, Shaw J, Lacomme C, Schweizer P, Duchkov D, Hensel G, Kumlehn J, Huckelhoven R (2010) BAX INHIBITOR-1 is required for full susceptibility of barley to powdery mildew. Mol Plant Microbe Interact 23:1217–1227

Fukuchi-Mizutani M, Tasaka Y, Tanaka Y, Ashikari T, Kusumi T, Murata N (1998) Characterization of Δ9 acyl-lipid desaturase homologues from *Arabidopsis thaliana*. Plant Cell Physiol 39:247–253

Ihara-Ohori Y, Nagano M, Muto S, Uchimiya H, Kawai-Yamada M (2007) Cell death suppressor, *Arabidopsis* BI-1, is associated with calmodulin-binding and ion homeostasis. Plant Physiol 143:650–660

Ikeyama Y, Tasaka M, Fukaki H (2010) RLF, a cytochrome $b_5$-like heme/steroid binding domain protein, controls lateral root formation independently of ARF7/19-mediated auxin signaling in *Arabidopsis thaliana*. Plant J 62:865–875

Imari J, Baltruschat H, Stein E, Jia G, Vogelsberg J, Kogel KH, Hückelhoven R (2006) Expression of barley BAX Inhibitor-1 in carrots confers resistance to *Botrytis cinerea*. Mol Plant Pathol 7:279–284

Ishikawa T, Takahara K, Hirabayashi T, Matsumura H, Fujisawa S, Terauchi R, Uchimiya H, Kawai-Yamada M (2010) Metabolome analysis of response to oxidative stress in rice suspension cells overexpressing cell death suppressor Bax inhibitor-1. Plant Cell Physiol 51:9–20

Ishikawa T, Watanabe N, Nagano M, Kawai-Yamada M, Lam E (2011) Bax inhibitor-1: a highly conserved endoplasmic reticulum-resident cell death suppressor. Cell Death Differ 18:1271–1278

Ishikawa T, Uchimiya H, Kawai-Yamada M (2013) The role of plant Bax inhibitor-1 in suppressing $H_2O_2$-induced cell death. Methods Enzymol 527:239–256

Kawai M, Pan L, Reed JC, Uchimiya H (1999) Evolutionally conserved plant homologue of the Bax inhibitor-1 (BI-1) gene capable of suppressing Bax-induced cell death in yeast. FEBS Lett 464:143–147

Kawai-Yamada M, Jin L, Yoshinaga K, Hirata A, Uchimiya H (2001) Mammalian Bax-induced plant cell death can be down-regulated by overexpression of *Arabidopsis* Bax Inhibitor-1 (AtBI-1). Proc Natl Acad Sci USA 9:12295–12300

Kawai-Yamada M, Ohori Y, Uchimiya H (2004) Dissection of *Arabidopsis* Bax Inhibitor-1 suppressing Bax-, hydrogen peroxide-, and salicylic acid-induced cell death. Plant Cell 16:21–32

Kawai-Yamada M, Hori Z, Ihara-Ohori Y, Tamura K, Nagano M, Ishikawa T, Uchimiya H (2009) Loss of calmodulin binding to Bax inhibitor-1 affects *Pseudomonas*-mediated hypersensitive response-associated cell death in *Arabidopsis thaliana*. J Biol Chem 284:27998–28003

Kim MC, Panstruga R, Elliott C, Muller J, Devoto A, Yoon HW, Park HC, Cho MJ, Schulze-Lefert P (2002) Calmodulin interacts with MLO protein to regulate defense against mildew in barley. Nature 416:447–450

Liang H, Yao N, Song JT, Luo S, Lu H, Greenberg JT (2003) Ceramides modulate programmed cell death in plants. Genes Dev 17:2636–2641

Maggio C, Barbante A, Ferro F, Frigerio L, Pedrazzini E (2007) Intracellular sorting of the tail-anchored protein cytochrome *b*5 in plants: a comparative study using different isoforms from rabbit and *Arabidopsis*. J Exp Bot 58:1365–1379

Markham JE, Jaworski JG (2007) Rapid measurement of sphingolipids from *Arabidopsis thaliana* by reversed-phase high-performance liquid chromatography coupled to electrospray ionization tandem mass spectrometry. Rapid Commun Mass Spectrom 21:1304–1314

Markham JE, Li J, Cahoon EB, Jaworski JG (2006) Separation and identification of major plant sphingolipid classes from leaves. J Biol Chem 281:22684–22694

Markham JE, Lynch DV, Napier JA, Dunn TM, Cahoon EB (2013) Plant sphingolipids: function follows form. Curr Opin Plant Biol 16:350–357

Matsumura H, Sm Nirasawa, Kiba A, Urasaki N, Saktoh H, Ito M, Kawai-Yamada M, Uchimiya H, Terauchi R (2003) Overexpression of Bax inhibitor suppresses the fungal elicitor-induced cell death in rice (*Oryza sativa* L.) cells. Plant J 33:425–434

Mendel RR (2011) Cell biology of molybdenum in plants. Plant Cell Rep 30:1787–1797

Minami A, Furuto A, Uemura M (2010) Dynamic compositional changes of detergent-resistant plasma membrane microdomains during plant cold acclimation. Plant Signal Behav 5:1115–1118

Miura K, Furumoto T (2013) Cold signaling and cold response in plants. Int J Mol Sci 14:5312–5337

Mizutani M (2012) Impacts of diversification of cytochrome P450 on plant metabolism. Biol Pharm Bull 35:824–832

Nagano M, Ihara-Ohori Y, Imai H, Inada N, Fujimoto M, Tsutsumi N, Uchimiya H, Kawai-Yamada M (2009) Functional association of cell death suppressor, *Arabidopsis* Bax inhibitor-1, with fatty acid 2-hydroxylation through cytochrome $b_5$. Plant J 17:122–134

Nagano M, Takahara K, Fujimoto M, Tsutsumi N, Uchimiya H, Kawai-Yamada M (2012) *Arabidopsis* sphingolipid fatty acid 2-hydroxylases (AtFAH1 and AtFAH2) are functionally differentiated in fatty acid 2-hydroxylation and stress responses. Plant Physiol 159:1138–1148

Nakagawa T, Suzuki T, Nakamura S, Hino T, Maeo K, Tabata T, Kawai T, Tanaka K, Niwa Y, Watanabe Y, Nakamura K, Kimura T, Ishiguro S (2007) Improved Gateway binary vectors: high-performance vectors for creation of fusion constructs in transgenic analysis of plants. Biosci Biotech Biochem 71:2091–2100

Nishida I, Murata N (1996) Chilling sensitivity in plants and cyanobacteria: the crucial contribution of membrane lipids. Annu Rev Plant Mol Biol 47:541–568

Pata MO, Hannun YA, Ng CK (2010) Plant sphingolipids: decoding the enigma of the Sphinx. New Phytol. 185:611–630

Sanchez P, de Torres-Zabala M, Grant M (2000) AtBI-1, a plant homologue of Bax inhibitor-1, suppresses Bax-induced cell death in yeast and is rapidly upregulated during wounding and pathogen challenge. Plant J 21:393–399

Schenkman JB, Jansson I (2003) The many roles of cytochrome $b_5$. Pharmacol Ther 97:139–152

Smith MA, Dauk M, Ramadan H, Yang H, Seamons LE, Haslam RP, Beaudoin F, Ramirez-Erosa I, Forseille L (2013) Involvement of *Arabidopsis* ACYL-COENZYME A DESATURASE-LIKE2 (At2g31360) in the biosynthesis of the very-long-chain monounsaturated fatty acid components of membrane lipids. Plant Physiol 161:81–96

Spassieva SD, Markham JE, Hille J (2002) The plant disease resistance gene *Asc-1* prevents disruption of sphingolipid metabolism during AAL-toxin-induced programmed cell death. Plant J 32:561–572

Sperling P, Schmidt H, Heinz E (1995) A cytochrome-$b_5$-containing fusion protein similar to plant acyl lipid desaturases. Eur J Biochem 232:798–805

Sperling P, Zahringer U, Heinz E (1998) A sphingolipid desaturase from higher plants. J Biol Chem 30:28590–28596

Townley HE, McDonald K, Jenkins GI, Knight MR, Leaver CJ (2005) Ceramides induce programmed cell death in *Arabidopsis* cells in a calcium-dependent manner. Biol Chem 386:161–166

Uemura M, Joseph RA, Steponkus PL (1995) Cold acclimation of Arabidopsis thaliana (Effect on plasma membrane lipid composition and freeze-induced lesions). Plant Physiol 109:15–30

Upchurch RG (2008) Fatty acid unsaturation, mobilization, and regulation in the response of plants to stress. Biotechnol Lett 30:967–977

Watanabe N, Lam E (2006) *Arabidopsis* Bax inhibitor-1 functions as an attenuator of biotic and abiotic types of cell death. Plant J 45:884–894

Watanabe N, Lam E (2008) BAX inhibitor-1 modulates endoplasmic reticulum stress-mediated programmed cell death in *Arabidopsis*. J Biol Chem 283:3200–3210

Weis C, Pfeilmeier S, Glawischnig E, Isono E, Pachl F, Hahne H, Kuster B, Eichmann R, Huckelhoen R (2013) Co-immunoprecipitation-based identification of putative BAX INHIBITOR-1-interacting proteins involved in cell death regulation and plant-powdery mildew interactions. Mol Plant Pathol 14:791–802

Wittke S, Lewke N, Muller S, Johnsson N (1999) Probing the molecular environmental of membrane proteins in vivo. Mol Biol Cell 10:2519–2530

Xu Q, Reed JC (1998) Bax inhibitor-1, a mammalian apoptotic suppressor identified by the functional screening in yeast. Mol Cell 1(3):337–346

Yue H, Nie S, Xing D (2012) Over-expression of *Arabidopsis* Bax inhibitor-1 delays methyl jasmonate-induced leaf senescence by suppressing the activation of MAP kinase 6. J Exp Bot 63:4463–4474

Zhao J, Onduka T, Kinoshita JY, Honsho M, Kinoshita T, Shimazaki K, Ito A (2003) Dual subcellular distribution of cytochrome $b_5$ in plants, cauliflower, cells. J Biochem 133:115–121